Dielectric Behavior Of Water In [bmim] [Tf2N] Room-Temperature Ionic Liquid, Molecular Dynamic Study.

Raúl Fuentes-Azcatl (razcatl@xanum.uam.mx)
Universidade Federal Fluminense https://orcid.org/0000-0001-8645-9506
Gabriel J. C. Araujo
Universidade Federal Fluminense
Tuanan C. Lourenço
Universidade Federal Fluminense
Cauê T. O. G. Costa
Universidade Federal Fluminense
José Walkimar de M. Carneiro
Universidade Federal Fluminense
Luciano T. Costa
Universidade Federal Fluminense

Research Article

Keywords: Dielectric constant, Water Structure, Dipole Moment average, Polarizable water

Posted Date: April 26th, 2021

DOI: https://doi.org/10.21203/rs.3.rs-415686/v1

Dielectric behavior of Water in [bmim] [Tf_2N] room-temperature Ionic Liquid, molecular dynamic study.

Raúl Fuentes-Azcatl,* Gabriel J. C. Araujo, Tuanan C. Lourenço, Cauê T. O. G. Costa, José Walkimar de M. Carneiro, and Luciano T. Costa*

Instituto de Química, Universidade Federal Fluminense-Outeiro de São João Batista, s/n CEP:24020-141, Niterói, RJ, Brazil

E-mail: razcatl@correo.xoc.uam.mx; ltcosta@id.uff.br

Abstract

In this work we present the dielectric behavior of water with a novel flexible model that improved all three sites water models Different concentrations of the ionic liquid 1-butyl-3-methylimidazolium [bmim] bis(trifluoromethanesulfonyl)imide [Tf_2N] with water was investigated. The study was performed by molecular dynamics simulations using three water models, being two non-polarizable 3-site SPC/E and SPC/e, and a novel flexible 3-site FAB/ϵ model. Systematic thermodynamics, dynamical and dielectric properties were investigated, such as density, diffusion coefficient, heat of vaporization ΔHvap, and surface tension at 300 K and 1 bar. We extrapolated the experimental molar fraction of the mixtures and a pattern change for all properties was observed, evidencing the phase separation previously reported by experimental data. The results also display the dielectric effect of the system on the calculated properties.

Keywords

Dielectric constant, Water Structure, Dipole Moment average, Polarizable water.

Introduction

Ionic Liquids (ILs) have been investigated widely in the last years, with applications being reported since the early 20th century. For instance, ILs were applied to cellulose dissolution in 1930s, when a pattent described the use of a molten pyridinium salt for this purpose.[1]

Ionic liquids have great capacity to dissolve an extensive group of polar and non-polar compounds,making them a desirable solvent for many applications, such as catalysis,[2–4] extraction,[5,6] self-assembly,[7–12] electrochemical[13–15] and biochemical processes.[16–18]

The search for new anions for organic polymer electrolytes raised the concept of a "plasticizing anion", i.e., an anion with delocalized charge and multiple conformations which differ in energy only slightly. One example of this is the anion bis (trifluoromethanelsulphonyl) imide $[CF_3SO_2\text{-}N\text{-}SO_2CF_3]^+$, also known as $[Tf_2N]^-$. It was shown that this anion, together

with imidazolium cations such as [bmim][Tf_2N], forms an IL with a melting point around 288 K, ionic conductivity comparable to that of good organic electrolyte solutions[1] and no decomposition or significant vapour pressure up to 550-650K.[19]

It is well known that the water content can disrupt and strongly affect the ionic liquids properties .[21,22] For instance water has an important role in the dissolution of cellulose in ILs, revealing the importance of hydrogen bonds making and disrupting environment. Recently, McDaniel and Verma studied the miscibility of ILs in water and showed the dependence of the dielectric medium based on ion type and cation/anion combination .[23] [bmim][Tf_2N] is not miscible with water, presenting a solubility around 1,000 p.p.m. in aqueous solutions.[1] Imidazolium based ILs and anions like [Tf_2N] form biphasic systems with water, being used in separation processes. [24] Due to that, the dielectric behavior of [bmim][Tf_2N] in water becomes an interesting system to be explored. Even with some aspects being already investigated in the literature ,[25] others still remain.

A determining condition for the study of ionic systems in aqueous solution, within computational theoretical studies based on molecular dynamics technique, is the choice of the force field. Since the last century, water force fields have been developed,[27,28,31,33] being the TIP4P family one of the most used for improving their ability to tackle with the polarization effects, reproducing better the experimental values at various pressure and temperature conditions.[27] Since Vega et al[27] proposed an equation which qualifies according to the experimental values and those reproduced by the model, it has been taken as a reference to qualify and develop new approaches for water force fields.[20,31]

As described by Vega et al,[27] until 2011 the water models failed with respect to the reproduction of dielectric properties that are determined by the dipole moment, inducing the development of various models since that year.,[28,31,33] which has contributed to having better monovalent salt[29,30]force fields. The FAB/ϵ model reproduces more and better various experimental values.[31] An advantage of the FAB/ϵ model over the other ones is related to its flexibility, helping to understand how the structure of water changes within a solution.

In the present work we employ this model to study a water/IL mixture by the first time.

In the literature there are several force fields for [bmim][Tf_2N], which have been established by the reproduction of some experimental property, such as density, X-ray structure factors, self-diffusion coefficients from NMR and heats of vaporization from vapor pressure measurements.[34] The first force fields were obtained from ab initio[36] methods and compared with the reproduction of the liquid density. Currently there are more experimental data and therefore conditions to improve the IL force field.[34]

The remaining of the paper goes as follows. In section 2 we introduce the models. Section 3 shows the simulation details. The results are analysed in Section 4. Conclusions are presented in section 5.

Computational Details and Models

Force Fields

Three different Force Fields (FF) for water were used to investigate the effects on the ionic liquid properties, varying the water content. The SPC/E,[32] a non-polarizable model which is widely applied, the SPC/ϵ[33] model, an improvement of SPC model with new Lennard-Jones and charges parameters, and the FAB/ϵ[31] model, a flexible 3-site model which can reproduce various thermodynamic properties at different conditions and improve the 3-sites water model.

All these models have 3 point charges centered on each atom and a Lennard-Jones site for the oxygen. Table 1 shows the force field parameters for the three models.

Table 1: Parameters of the three-site water models considered in this work.

model	k_b	r_{OH}	k_a	Θ	ε_{OO}	σ_{OO}	q_O	q_H
	kJ/ *mol* Å^2	Å	kJ/ *mol* rad^2	deg	kJ/mol	Å	e	e
SPC/E[32]	-	1.000	-	109.45	0.650155	3.1660	-0.8476	0.4238
SPC/ϵ[33]	-	1.000	-	109.45	0.705859	3.1785	-0.8900	0.4450
FBA/ϵ[31]	3000	1.027	383	114.70	0.792324	3.1776	-0.8450	0.4225

In general, non-polarizable models have the Lennard-Jones and Coulomb potentials to describe the intermolecular interactions as follows:

$$u(r) = 4\epsilon_{\alpha\beta}\left[\left(\frac{\sigma_{\alpha\beta}}{r}\right)^{12} - \left(\frac{\sigma_{\alpha\beta}}{r}\right)^{6}\right] + \frac{1}{4\pi\epsilon_0}\frac{q_\alpha q_\beta}{r} \tag{1}$$

where α and β refers to atomic sites, r is the distance between the sites α and β, q_α and q_β accounts to the electric charges for the sites α and β, respectively; ϵ_0 is the vacuum permittivity, $\epsilon_{\alpha\beta}$ is the LJ energy scale and $\sigma_{\alpha\beta}$ is the repulsive diameter for an $\alpha - \beta$ pair. The cross interactions between different atoms are obtained using the Lorentz-Berthelot mixing rules,

$$\sigma_{\alpha\beta} = \left(\frac{\sigma_{\alpha\alpha} + \sigma_{\beta\beta}}{2}\right); \qquad \epsilon_{\alpha\beta} = \left(\epsilon_{\alpha\alpha}\epsilon_{\beta\beta}\right)^{1/2} \tag{2}$$

The FAB/ϵ model includes two harmonic potential,that improve the calculation of experimental properties,[35] one at the OH bond and another at the angle formed by the three atoms of a water molecule, as shown in the Equations 3 and 4:

$$U_k(r) = \frac{k_r}{2}(r - r_0)^2 \tag{3}$$

$$U_\theta(\theta) = \frac{k_\theta}{2}(\theta - \theta_0)^2, \tag{4}$$

where r is the bond distance and θ is the bond angle. The subscript 0 denotes their equilibrium values, while k_r and k_θ are the corresponding spring constants.

Figure 1 exhibits the molecule model for the ions in the IL [bmim][Tf_2N], with the cation on the rigth and the anion on the left side. For the IL, the united atom force field proposed by K*ö*ddermann et. al[34] was used.

In this FF, hydrogen atoms are not explicitly placed and their contribution is included in the atom to which it is bound. However, carbon atoms in the aromatic ring have an explicit hydrogen, taken into account by placing an atom with specific characteristics according to the position where it is found. Also the energetic contribution of the fluorine atoms bonded to the carbons in Tf_2N anion are included in the corresponding carbon atom.

Simulation Details

Molecular Dynamics (MD) simulations on the liquid phase for binary mixtures were performed using the isothermal-isobaric (NpT) ensemble[37] to obtain the density, the dielectric constant, the self-diffusion coefficient and the heat of vaporization. For this purpose the Gromacs package was used.[38] A total of 864 molecules were used in all simulations performed. The leapfrog equations of motion were solved with a time step of 1 fs. Periodic boundary

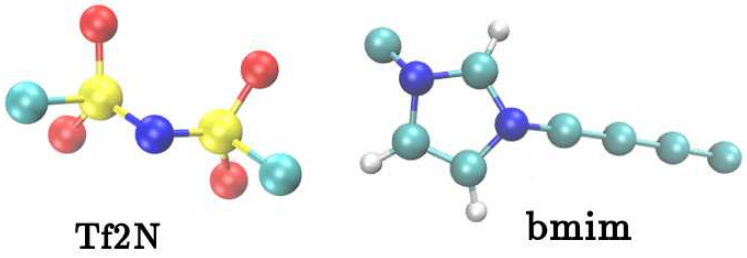

Figure 1: The cyan spheres represent a Carbon atom, red spheres a Oxygen atom, blue spheres a Sodium atom, yellow spheres a Sulfur atom and white spheres Hidrogen (only the carbons at the aromatic ring have an explicit hidrogen), the contribution of the other Hydrogen atoms is contained in the respective carbons, as well as the contribution of the Fluorine atoms.

conditions were used in all the directions and the bond distances were kept rigid with the LINCS procedure,[39] when necessary. The cutoff distance applied was equal to 1.0 nm for both the real part of the Coulomb potential and the LJ interactions; In addition, analytical long-range corrections were applied for the second one. The PME method[42] was applied to evaluate the reciprocal contribution with a grid of 0.34 nm for the reciprocal vectors with a spline of order 4. The Nosé-Hoover thermostat and Parrinello-Rahman barostat were applied with the coupling times of 0.6 and 1.0 ps, respectively. The average properties were obtained after a production runs of 50 ns long.

The water static dielectric constant, ϵ, is a collective property of an ensemble of water dipoles, which can be calculated from the equilibrium total dipole moment fluctuations, $(< \mathbf{M}^2 > - < \mathbf{M} >^2)$. The calculations of the dielectric constant was obtained by (equation 5)[40] of the total dipole moment $\mathbf{M}$,

$$\epsilon = 1 + \frac{4\pi}{3k_B TV}(< \mathbf{M}^2 > - < \mathbf{M} >^2) \tag{5}$$

where k_B is the Boltzmann constant, T is the absolute temperature and V is the volume.

The surface tension was obtained in a NVT simulation where a rectangular cell was used, with L_x=L_y=7.9 nm and $L_z = 3L_x$ to avoid finite effects,[41] containing 5324 molecules. Periodic boundary conditions were applied in all directions.

The average components of the pressure tensor were obtained for 30 ns after an equilibration period of 5 ns. The densities of the two phases were extracted from the statistical averages of the liquid and vapor limits of the density profiles.[43] The corresponding surface tension γ on the planar interface was calculated from the mechanical definition of γ .[43]

$$\gamma = 0.5L_z[< P_{zz} > -0.5(< P_{xx} > + < P_{yy} >)] \tag{6}$$

where L_z is the length of the simulation cell in the longest direction and $P_{\alpha\alpha}$ are the diagonal components of the pressure tensor. The factor 0.5 outside the squared brackets takes into account the two symmetrical interfaces in the system.

Results

Figure 2 shows the density of the IL-water system at different mole fraction of water X_{H2O}. Although the calculated density of the pure IL is underestimated in 2.68%, indicating that the force field for the IL can be improved, the behavior of the density using the three different force fields for water has a systematic decreasing. The inset (A) of the Figure 2 shows the equilibrated configuration at the fraction of X_{H2O}=0.95, where a non-homogeneous mixture is evidenced, suggested previously by Rollet et al.[25]

The density of the IL-water system (figure 2) with respect to an increment of X_{H2O} decreases by 40% until reaching a composition of pure water; the density obtained with the FAB/ϵ model shows lower values than those obtained when using the non-polarizable models, within the region from X_{H2O}=0.2 to X_{H2O}=0.8. This is due to the contracting ability of the OH bond in the water molecule, as will be analyzed and discussed in the average structure of the water molecules in the system IL-water in this work.

Figure 3A exhibits the results of the dielectric constant of the IL-water system for the three models studied. The difference between the water models is closer to the pure water, where the dielectric derived models present a better agreement to the experimental data.

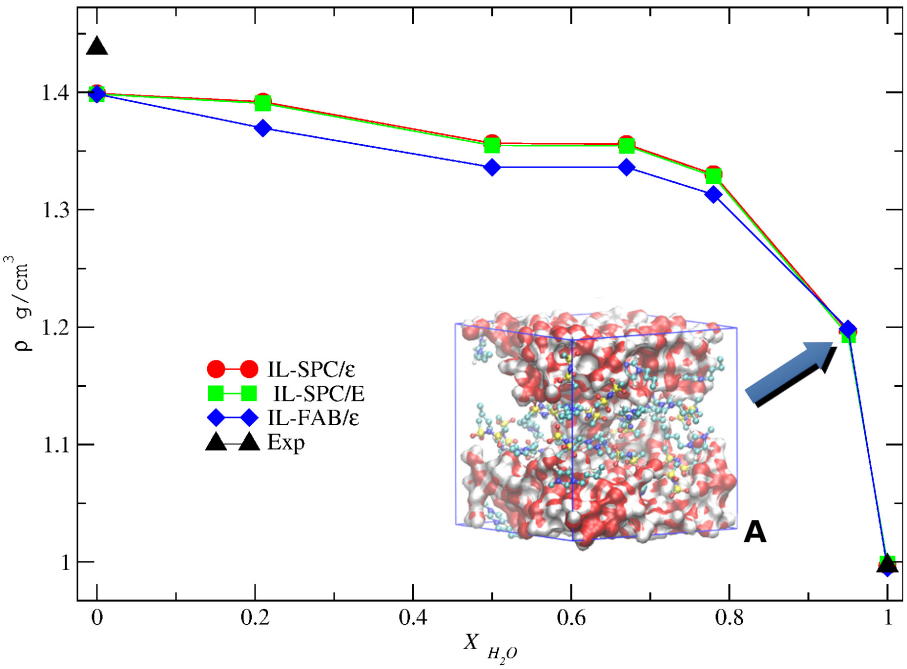

Figure 2: Density of the water-IL solution as function of the molar fraction of water at 1 bar of pressure. Black triangles are the experimental data,[44] red circles are the result using the SPC/ϵ model, green box are the result using the SPC/E model, and the blue dimonds are the result using FAB/ϵ model, all calculated in this work.

Following the previous trend, the IL force field understimate the dielectric constant of the neat IL. The dielectric constant of the system can be reduced up to 60%, when compared to pure water, even with a small amount of the IL. However, the system has a monotonic behavior for molar fractions of water lower than 80%. Figure 3A shows the dielectric constant of the IL in the system.

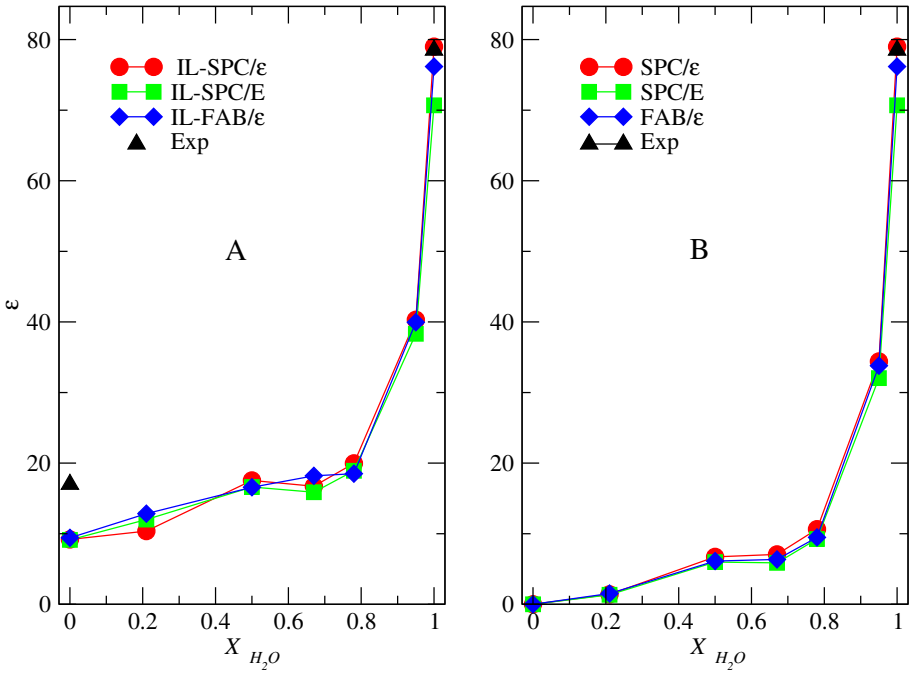

Figure 3: **A**: Dielectric constant of the water-IL solution as function of the molar fraction of water. **B**: Dielectric constant of the water in the IL-water solution as function of the molar fraction of water. Both at 1 bar of pressure and 298 K of temperature. Black triangles are the experimental data,[45] red circles are the result using the SPC/ϵ model, green box are the result using the SPC/E model and the blue dimonds are the result using FAB/ϵ model, all calculated in this work.

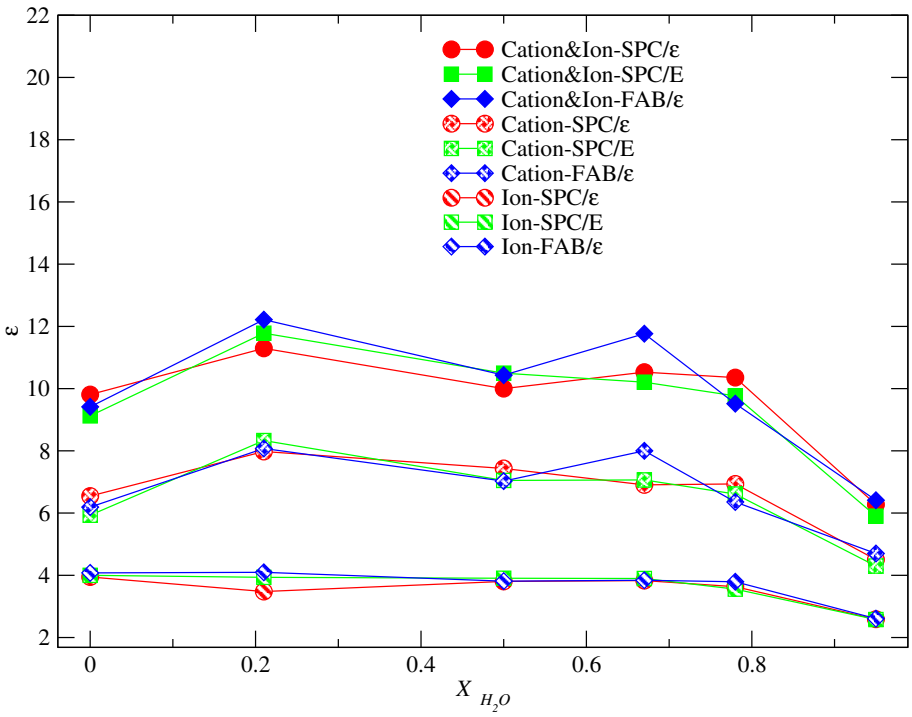

Figure 4: Dielectric constant of the IL, cation and anion in the water-IL solution as function of the molar fraction of water at 1 bar of pressure.

Analizing the dielectric constant of water in the solution, Figure 3B, it can be seen that the three water models show an identical description of this property. However, the FAB/ϵ model has the advantage of giving more information on the structural behavior of figures6, 7 and 8.

Figure 4 shows the behavior of the anion, cation and both in the IL-water system. The anion remains within a constant range, even when the amount of water in the system increases and the cation presents variations within a percentage of 20% with respect to the absence of water. Thus the cation with this model has more reactivity than the anion.

The static dielectric constant, ε, of a polar liquid is related to the thermal equilibrium fluctuations of the polarization at zero field.[46] Polarization fluctuations are long-range and vary with the shape of the dielectric body. ε, on the other hand, is an intrinsic response coefficient independent of geometry. This led Kirkwood to postulate that it should be possible to express ε in terms of a short-range orientational correlation function.[47]

The values of the polarization of simulation is presented in the figure 5. We introduce

the polarisation factor G_K (equation 7),[49] in order to check if the force field changes its polarisation; the G_K factor measures the equilibrium fluctuations of the collective dipole moment of the system and is related to the orientational correlation function.. The calculus of the polarization is consistent for the three water models, including the polarizable FAB/ε model, which implies that the system is consistently reproduced by these water models, and that water also governs the polarization of the system. By having a small amount of water in the system, it becomes more polarized and this causes its dielectric properties to increase, even when the system is not miscible.

The result is consistent with the three water models, Figure 5, which indicates that a water model that does not reproduce the dielectric constant well, will not reproduce this behaivor, as shown in the work of Schröder et al[50]

$$G_K =< \mathbf{M}^2 > /N\mu^2 \tag{7}$$

N is the total number of molecules, M is the total sum of dipoles μ_i in the system (including the dipole of initial molecule). Local orientational correlations are averaged out by thermal motion after the first few coordination shells.

Even though the result of the dielectric constant and the polarization of water in the system with IL is consistent, the use of the new force field generates structural information on the behavior of water through the dipole moment, as seen in the figure 6. The average dipole moment of water, when increase its quantity with respect to IL, show water changes structurally with an angle less than isolated water, when it is closer to the IL. And by not being in contact with IL, it again deploys to a state of bulk.

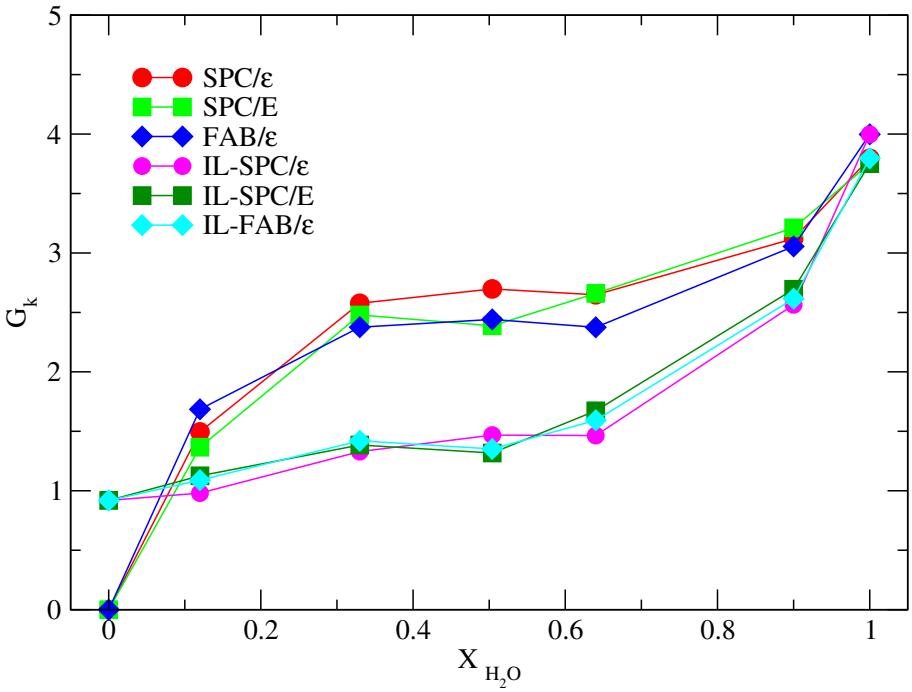

Figure 5: Kirkwood factor G_K of the water in the IL-water solution and for all solution as function of the molar fraction of water at 1 bar of pressure and 300K. Red circles are the result using the SPC/ϵ model, green box are the result using the SPC/E model and the blue dimonds are the result using FAB/ϵ model, all calculated in this work.

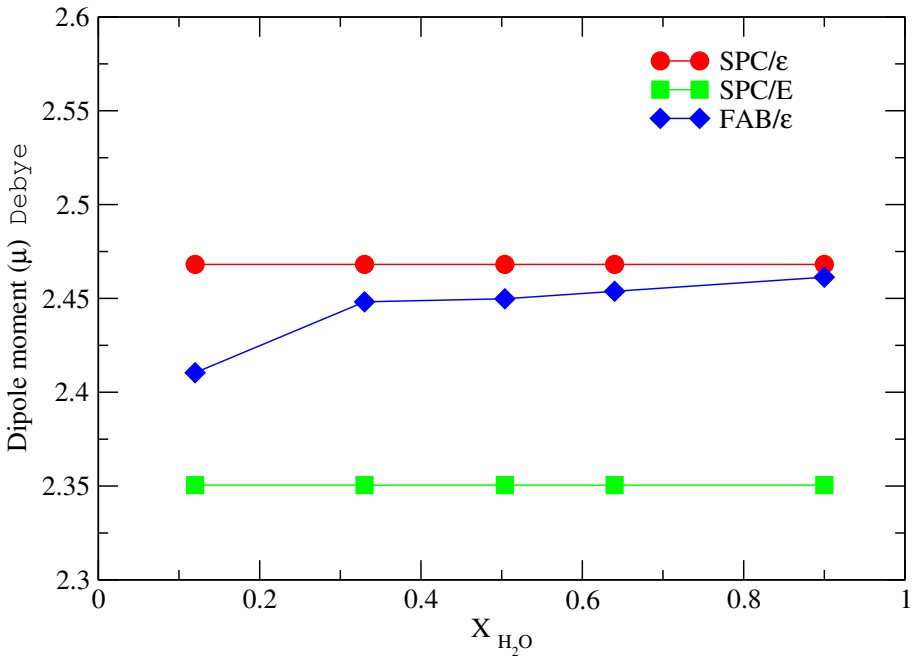

Figure 6: Dipole Moment of the water in the IL-water solution as function of the molar fraction of water at 1 bar of pressure and 300K. Red circles are the result using the SPC/ϵ model, green box are the result using the SPC/E model and the blue dimonds are the result using FAB/ϵ model, all calculated in this work.

The dipole moment is a function of the location of the charges in the molecules with respect to time. In the case of rigid molecules we have a restorative force that turns the molecule fixed; in the case of the FAB/ϵ model, we have the possibility of having a displacement with a certain freedom caused by the harmonic potential, both in the angle and in the OH bond, which makes the structure free. From there we can obtain a broad understanding of how the water molecule behaves through various concentrations within this IL study, figure 6.

The dipole moment increases with respect to the amount of water in the system, this is due to the fact that the angle decreases in this process, see figure 7, approaching the hydrogens in the molecule; however the bond distance between oxygen and hydrogen O-H $_{bond}$ also decreases, see figure 8, which makes the interaction in the molecule stronger due to the contraction it undergoes. Then, when it reaches the bulk of pure water the molecule is more compact and when it is in a small quantity with ionic liquid it relaxes expanding its

angle and O-H bond $_{bond}$

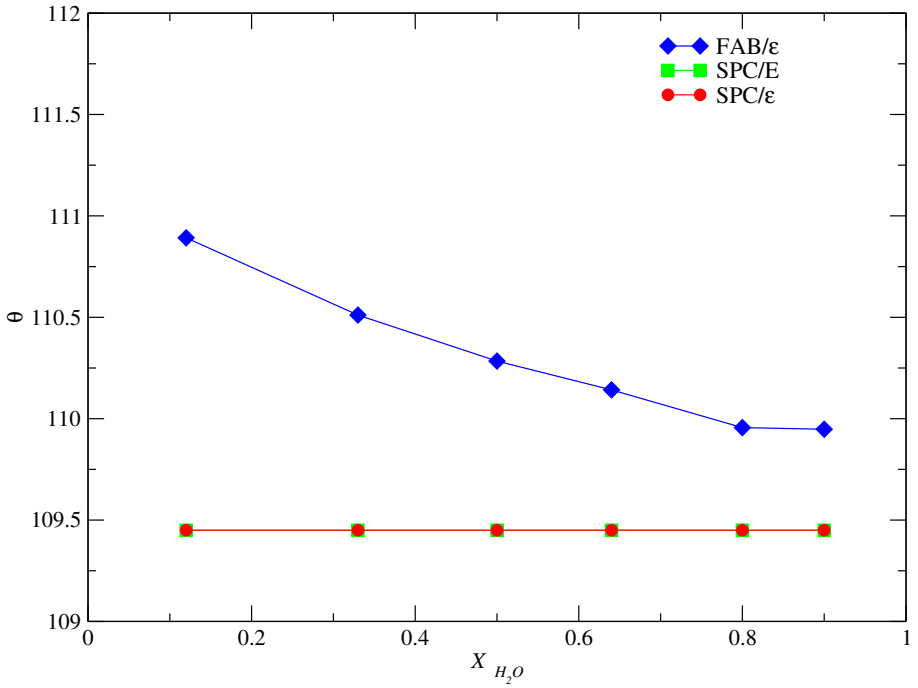

Figure 7: Average angle of the water described by the three force fields as function of the molar fraction of water at 1 bar of pressure and 300K. Red circles are the result using the SPC/ϵ model, green box are the result using the SPC/E model and the blue dimonds are the result using FAB/ϵ model, all calculated in this work.

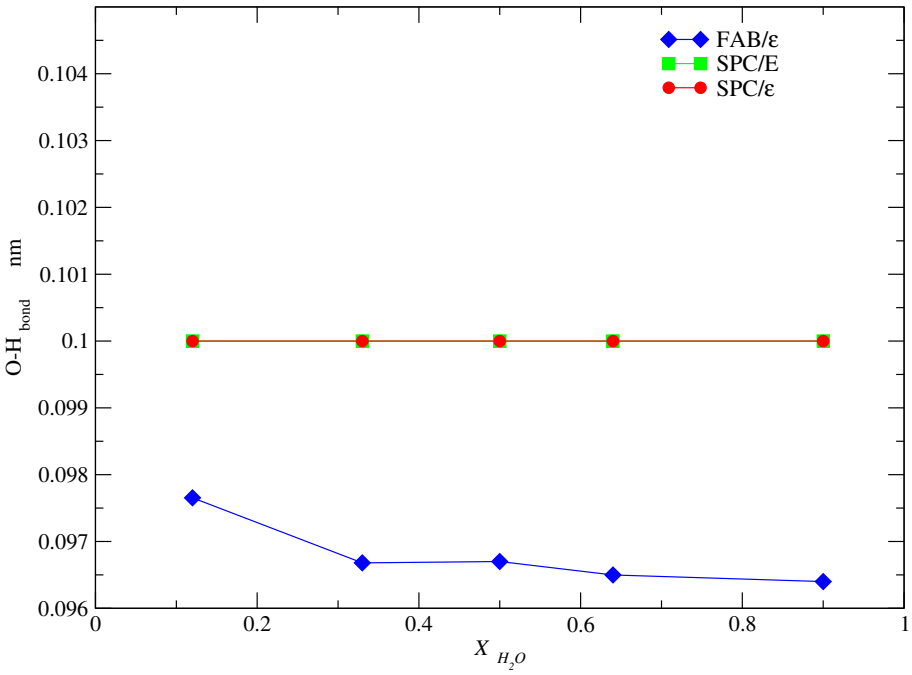

Figure 8: Average O-H_{bond} of the water described by the three force fields as function of the molar fraction of water at 1 bar of pressure and 300K. Red circles are the result using the SPC/ϵ model, green box are the result using the SPC/E model and the blue dimonds are the result using FAB/ϵ model, all calculated in this work.

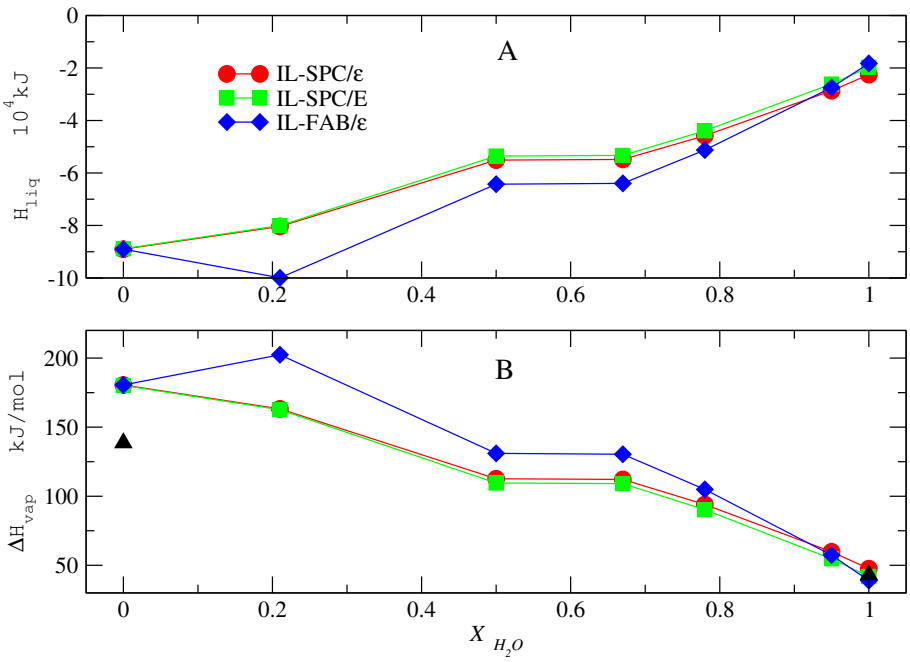

Figure 9: **A**. Enthalpy of the liquid phase the IL-water solution as function of the molar fraction of water. **B**. △Hvap of the system with respect to the fraction of water in the solution IL-water. Both at 1 bar of pressure and 300K of temperature. Black triangles are the experimental data,[48] red circles are the result using the SPC/ϵ model, green box are the result using the SPC/E model and the blue dimonds are the result using FAB/ϵ model, all calculated in this work.

The analysis of the enthalpy of the liquid phase (Figure 9A), as we increase the amount of water in the solution, shows a decrease that stabilizes within a composition between 0.5 to 0.64 of the fraction of water. Outside that range there is a linear increase in the enthalpy.

The △Hvap of the system(Figure 9B) has a linear behavior outside the range of 0.5 to 6.4 of the fraction of water. Since the force field of IL underestimates the value of △Hvap of pure IL, the value calculated with the FAB water model might seem wrong, but having a calculation of pure water closer to experimental allows us to infer that the work must focus on a better force field of the IL , in order to have a better description of this property.

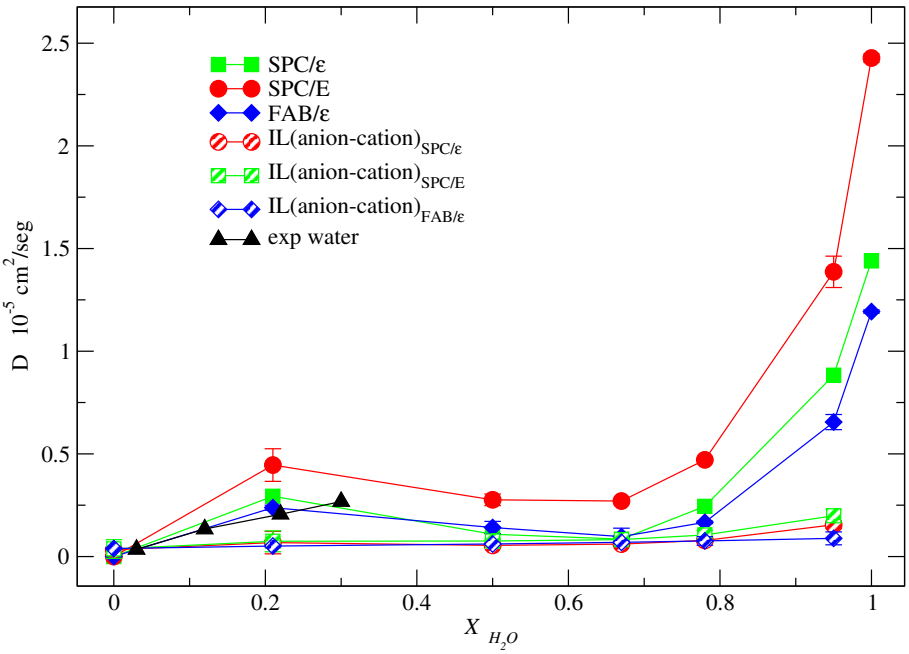

Figure 10: The self-diffusion coefficients of water and the IL with respect to the fraction of water in the solution IL-water. Black triangles are the experimental data,[25] red circles are the result using the SPC/ϵ model, green box are the result using the SPC/E model and the blue dimonds are the result using FAB/ϵ model, all calculated in this work.

The self-diffusion coefficients of water is show in Figure 10. When the water mol fraction is 0.2 in the solution, we have a description close to the experimental value of the diffusion, which describes the three water models, where the combination of IL-FAB/ϵ describes this behavior closer to the experiment. Then there is a decrease indicated by the three systems until the system reach the value that every water model reproduce at 1 bar and 298K. Taking

into account that IL is somewhat hygroscopic and not very miscible in water, the value it contains is 1.3[25] percent by mass, at the pressure and temperature conditions used.

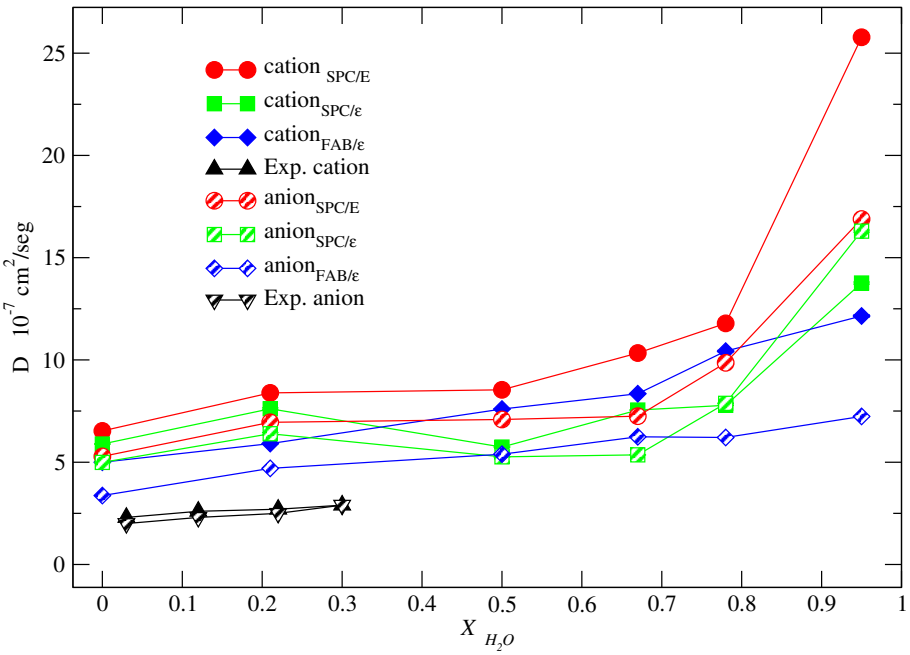

Figure 11: The self-diffusion coefficients of anion and the cation with respect to the fraction of water in the solution IL-water. Black triangles are the experimental data,[25] red circles are the result using the SPC/ϵ model, green box are the result using the SPC/E model and the blue dimonds are the result using FAB/ϵ model, all calculated in this work.

The self-diffusion coefficients of cation and anion is described by the Figure 11. Although the diffusion is almost equal for both according to the reported experimental value,[25] the calculated values that were obteined with the FBA/ϵ model are closer to the experimental values. Self-diffusion coefficient result is interesting, since IL is expected to be a little hygroscopic, so that water increases the dissociation rate of the ion pair and consequently causes a higher diffusion increase mainly from the anion, due to its size. When the amount of water is high, the diffusion of both is greater by a factor 1.3 than when there is less amount of water. These calculations show that increasing the water in the system does not produce a significant increased dissociation of the anion-cation pair, that is, it appears that water interacts rather weakly with the ion pair. Heinz et al[?] discuss how the water content depends on the interaction with the anion. The hydrophobicity of anions [NTf_2] prevents the water from dissociating ion pairs and incorporates more between the IL.

The surface tension of the system when the water is increased is show in the Figure 12.

Although the SPC/E model diverges from the experimental value by almost 12% at 300K and 1 bar, there is a similar behaivor since we started adding water to pure IL, until the increase reaches a mole fraction of 0.9 water. With a small amount of water, (χ_{H_20}= 0.12), the system decreases in value by almost 50%, which may be attributable to the fact that the IL force field does not describe this property well. From $\chi_{H_20} = 0.32$ to $\chi_{H_20} = 0.8$ we notice a similar behavior of the system, with small additions of water the system increases its value widely.

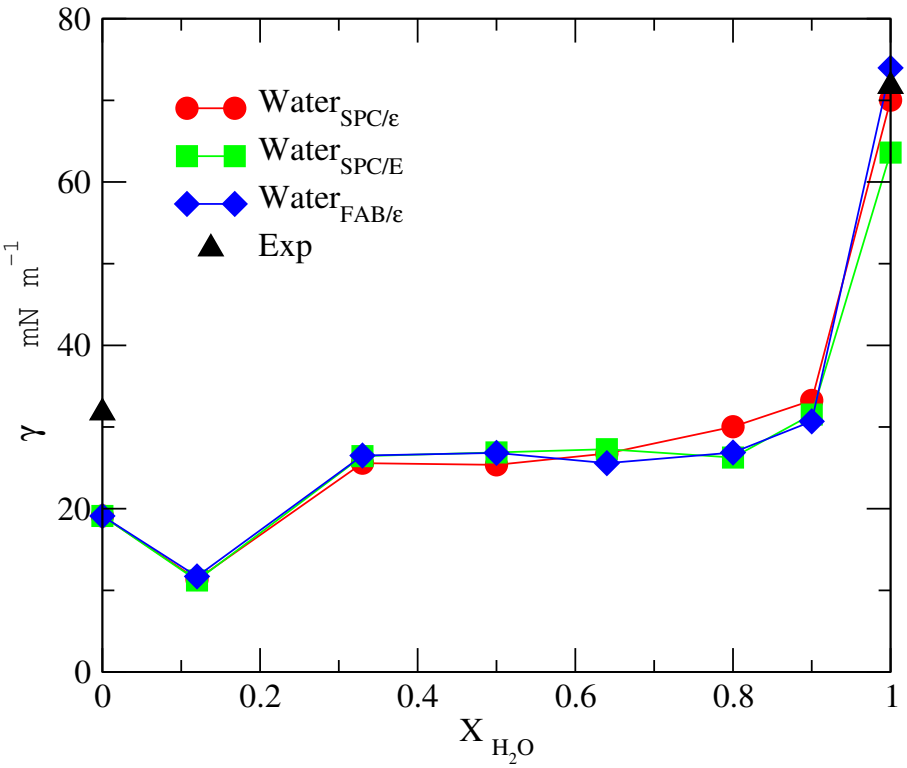

Figure 12: The surface tension of the system with respect to the fraction of water in the solution IL-water. Black triangles are the experimental data,[25] red circles are the result using the SPC/ϵ model, green box are the result using the SPC/E model and the blue dimonds are the result using FAB/ϵ model, all calculated in this work.

Conclusions

The novel flexible water FAB gives a novel information on how water is structured in these systems and how its dipole moment changes, this helps to understand water with IL that does not solubilize, giving a guideline to improve IL. The three water models used in this work together with IL reproduce the experimental properties of the system from a small amount of water to pure water. The fact that the FAB/ϵ model can change its structure within the simulation, generating a type of polarization, allows us to have a descriptive aspect of how the water molecule behaves through increasing its presence in the system, giving an important description to what other force fields can not do. This work shows the behavior and evolution of the three species [BMIM] [Tf_2N] + water at different concentrations, theoretically describing the behavior where there is still no experimental data but hypotheses have already been made regarding the system in these areas. An important challenge is to improve the IL force field in order to have a model closer to the experimental data and to have more certainty in the intermediate calculations of the properties calculated here.

The dielectric behavior of water within IL, as we increase its content, is reflected in the dipole moment, which indicates how the charges are located with respect to the atoms that form the molecule, and this is generated by the average structure defined by the O-H_{bond} and angle, so the polarization of the water increases as its angle and O-H_{bond} decrease.

Acknowledgements

Luciano T. Costa, José Walkimar de M. Carneiro and Cauê T. O. G. Costa thanks the Brazilian Federal Agency for Support and Evaluation of Graduate Education (CAPES/Print/UFF grant number 88881.310460/2018-01) and also for the CNPq fellowship grant. RFA thank CAPES posdoc scholarships.

Compliance with Ethical Standards

Conflict of interests

There are no conflicts of interest to declare.

Availability of data and material

N/A

Code availability

N/A

Author Statement

Raúl Fuentes-Azcatl: Writing, Methodology, Reviewing and Editing.

Gabriel J. C. Araujo: Methodology.

Tuanan C. Lourenço: Methodology.

Cauê T. O. G. Costa: Funding.

José Walkimar de M. Carneiro: Funding and Reviewing.

Luciano T. Costa: Funding and Reviewing.

References

(1) M. Armand, F. Endres, D. R. macFarlane, H. Ohno, B. Srosati, Ionic-liquid materials for the electrochemical challenges of the future. Nature Materials. **8**, 621 (2009).

(2) T. Welton, Room-temperature ionic liquids. Solvents for synthesis and catalysis, Chem. Rev. **99**, 2071 (1999).

(3) S. T. Keaveney, R. S. Haines and J. B. Harper, Developing principles for predicting ionic liquid effects on reaction outcome. The importance of the anion in controlling microscopic interactions, Org. Biomol. Chem. **12**, 3771 (2015).

(4) R. R. Hawker, R. S. Haines and J. B. Harper, The effect of varying the anion of an ionic liquid on the solvent effects on a nucleophilic aromatic substitution reaction, Org. Biomol. Chem. **18** 3453 (2018).

(5) J. F. Pereira, K. A. Kurnia, M. G. Freire, J. A. Coutinho and R. D. Rogers, Controlling the formation of ionic-liquid based aqueous biphasic systems by changing the hydrogen-bonding ability of polyethylene glycol end groups, Chem.Phys.Chem. **10**, 2219 (2015).

(6) J. F. B. Pereira, A. Magri, M. V. Quental, M. Gonzalez- Miquel, M. G. Freire and J. A. P. Coutinho, Alkaloids as alternative probes To characterize the relative hydrophobicity of aqueous biphasic systems, ACS Sustainable Chem.Eng. **3**, 1512 (2016).

(7) M. U. Araos and G. G. Warr, Self-assembly of nonionic surfactants into lyotropic liquid crystals in ethylammonium nitrate, a room-temperature ionic liquid, J. Phys.Chem. B, **109**, 14275 (2005).

(8) A. Dolan, R. Atkin and G. G. Warr, The origin of surfactant amphiphilicity and self-assembly in protic ionic liquids, Chem. Sci. **11**, 6189 (2015).

(9) T. Murphy, R. Hayes, S. Imberti, G. G. Warr and R. Atkin, Ionic liquid nanostructure enables alcohol self assembly, Phys. Chem. Chem. Phys. **18** 12797 (2016).

(10) T. L. Greaves, A. Weerawardena, C. Fong and C. J. Drummond, Formation of amphiphile self-assembly phases in protic ionic liquids, J. Phys. Chem. B. **111** 4082 (2007).

(11) Z. Chen, T. L. Greaves, C. Fong, R. A. Caruso and C. J. Drummond, Lyotropic liquid crystalline phase behaviour in amphiphile-protic ionic liquid systems, Phys. Chem. Chem. Phys. **11**, 3825 (2012).

(12) Z. Chen, T. L. Greaves, R. A. Caruso and C. J. Drummond, Amphiphile micelle structures in the protic ionic liquid ethylammonium nitrate and water, J. Phys. Chem. B, **119**, 179 (2015).

(13) T. Stettner, P. Huang, M. Goktas, P. Adelhelm and A. Balducci, Mixtures of glyme and aprotic-protic ionic liquids as electrolytes for energy storage devices, J. Chem. Phys. **148**, 193825 (2018).

(14) A. R. Neale, C. Schütter, P. Wilde, P. Goodrich, C. Hardacre, S. Passerini, A. Balducci and J. Jacquemin,Physical-chemical characterization of binary mixtures of 1-butyl-1-methylpyrrolidinium bis((trifluoromethyl)sulfonyl)imide and aliphatic nitrile solvents as potential electrolytes for electrochemical energy storage applications, J. Chem. Eng. Data. **62**, 376 (2016).

(15) M. Watanabe, M. L. Thomas, S. Zhang, K. Ueno, T. Yasuda and K. Dokko, Application of ionic liquids to energy storage and conversion materials and devices, Chem. Rev. **117**, 7190 (2017).

(16) M. Naushad, Z. A. Alothman, A. B. Khan and M. Ali, Effect of ionic liquid on activity, stability, and structure of enzymes: a review, Int. J. Biol. Macromol. **51**, 555 (2012).

(17) N. Byrne, J. P. Belieres and C. A. Angell, The 'Refoldability' of selected proteins in ionic liquids as a stabilization criterion, leading to a conjecture on biogenesis, Aust.J. Chem. **62**, 328 (2009).

(18) K. Fujita, D. R. MacFarlane and M. Forsyth, Protein solubilising and stabilising ionic liquids, Chem. Commun. 38 (2005) 4804-4806.

(19) M. J. Earle, J.M.S.S. Esperança, M.A. Gilea, J.N. Canongia, L.P.N. Rebelo, J.W. Magee, K.R. Seddon, J.A. Widegren, The distillation and volatility of ionic liquids. Nature **439**, 831 (2006).

(20) R. Fuentes-Azcatl, M.C. Barbosa, Thermodynamic and dynamic anomalous behavior in the TIP4P/ϵ water model, Physica A **444**, 86 (2016).

(21) A. Wulf, K. Fumino, R. Ludwig, Spectroscopic evidence for an enhanced anion–cation interaction from hydrogen bonding in pure imidazolium ionic liquids, Angew. Chem. Int. Ed. **49**, 449 (2010).

(22) T. Köddermann, C. Wertz, A. Heintz, R. Ludwig,The association of water in ionic liquids: a reliable measure of polarity, Angew. Chem. Int. Ed. **45**, 3697 (2006).

(23) J.G. McDaniel, A. Verma, On the miscibility and immiscibility of ionic liquids and water, J. Phys. Chem. B **123**, 5343 (2019).

(24) M.G. Freire, A.F.M. Cláudio, J.M.M. Araújo, J.A.P. Coutinho, I.M. Marrucho, J.N. Canongia, L.P.N. Rebelo, Chem. Soc. Rev. **41**, 4966 (2012).

(25) A.L. Rollet, P. Porion, M. Vaultier, I. Billard, M. Deschamps, C. Bessada, L. Jouvensal, Anomalous diffusion of water in [BMIM][TFSI] room-temperature ionic liquid. J. Phys.Chem. B, **111**, 11888 (2007).

(26) J. L. F. Abascal, C. Vega, A general purpose model for the condensed phases of water: TIP4P/2005, J. Chem. Phys. **123**, 234505 (2005).

(27) C. Vega, J. L. F. Abascal, Simulating water with rigid non-polarizable models: A general perspective. Phys. Chem. Chem. Phys. **13**, 19663 (2011).

(28) R. Fuentes-Azcatl, J. Alejandre, Non-polarizable force field of water based on the dielectric constant: TIP4p/ε, J. Phys. Chem. B. **118**, 1263 (2014).

(29) R. Fuentes-Azcatl, M.C. Barbosa, Sodium Chloride, NaCl/ϵ: New Force Field, J. Phys. Chem. B. **120**, 2460 (2016).

(30) R. Fuentes-Azcatl, M.C. Barbosa, Potassium bromide, KBr/ϵ: New Force Field, Physica A. **491**, 480 (2018).

(31) R. Fuentes-Azcatl, M.C. Barbosa, Flexible Bond and Angle, FBA/ε model of water model of water. Journal of Molecular Liquids. **303**, 112598 (2020).

(32) H.J.C. Berendsen, J.R. Grigera, T.P. Straatsma, The missing term in effective pair potentials, J. Phys. Chem. **91** 6269 (1987).

(33) R. Fuentes-Azcatl, N. Mendoza, J. Alejandre, Improved SPC force field of water based on the dielectric constant: SPC/ε. Physica A. **420**, 116 (2015).

(34) T. Köddermann, D. Paschek, R. Ludwig, Molecular dynamic simulations of ionic liquids: A reliable description of structure, thermodynamics and dynamics. Chem.Phys.Chem, **8**, 2464 (2007).

(35) R. Fuentes-Azcatl, H. Dominguez, Prediction of experimental properties of CO2: improving actual force fields, J. Mol. Modeling. **25**, 146 (2019).

(36) J.N.C. Lopes, J. Dechamps, A. A. H. Pódua, Modeling ionic liquids using a systematic all-atom force field, J. Phys. Chem. B. **108**, 2038 (2004).

(37) Tuckerman, M. E. Statistical Mechanics: Theory and Molecular Simulation; Oxford University Press, 2010.

(38) D. van der Spoel, E. Lindahl, B. Hess, G. Groenhof, A.E. Mark, H.C. Berendsen, GROMACS: fast, flexible, and free, J. Comput. Chem. **26**, 1701 (2005).

(39) B. Hess, C. Kutzner, D. van der Spoel, E. Lindahl, GROMACS 4.5 Algorithms for highly efficient, load-balanced, and scalable molecular simulation, J. Chem.Theory Comput. **4**, 435 (2008).

(40) M. Neumann, Dipole moment fluctuation formulas in computer simulations of polar systems. Mol. Phys. **50**, 841 (1983).

(41) P. Orea, J. Lopez-Lemus, J. Alejandre, J. Chem. Phys. **123**, 114702 (2005).

(42) U. Essmann, L. Perera, M.L. Berkowitz, T. Darden, H. Lee, L.G.J. Pedersen, A smooth particle mesh Ewald method J.Chem.Phys. **103**, 8577 (1995).

(43) J. Alejandre, D.J. Tildesley, G.A. Chapela, Molecular dynamics simulation of the orthobaric densities and surface tension of water, J. Chem. Phys. **102**, 4574 (1995).

(44) M.A.R. Martins, C.M.S.S. Neves, K.A. Kurnia, P.J. Carvalho, M.A.A. Rocha , L.M.N.B.F. Santos, S.P. Pinho, M.G. Freire, Densities, viscosities and derived thermophysical properties of water-saturated imidazolium-based ionic liquids, Fluid Phase Equilib. **407** 188 (2016).

(45) E. W. Lemmon, M.O. McLinden, D. G. Friend, Thermophysical properties of fluid systems, NIST Chemistry WebBook,NIST Standard Reference Database; P.J. Linstrom, W.G. Mallard, Eds.;2005; http://webbook.nist.gov (accessed February 1, 2020).

(46) H. Fröhlich, Theory of Dielectrics: Dielectric Constant and Dielectric Loss, 2nd ed.; Monographs on the physics and chemistry of materials; Oxford University Press: Oxford, 1958.

(47) Kirkwood, J. G. The Dielectric Polarization of Polar Liquids. J. Chem. Phys. **7**, 911 (1939).

(48) D. H. Zaitsau, G. J. Kabo, A. A. Strechnan, Y. U. Paulechka, A. Tschersich, S. P. Verevkin and A. Heintz, Experimental Vapor Pressures of 1-Alkyl-3-methylimidazolium Bis(trifluoromethylsulfonyl)imides and a Correlation Scheme for Estimation of Vaporization Enthalpies of Ionic Liquids, J. Phys. Chem. A **110**, 7303 (2006).

(49) A. Glattli, X. Daura and W. F. van Gunsteren, Derivation of an improved simple point charge model for liquid water: SPC/A and SPC/L, J. Chem. Phys. **116**, 9811 (2002).

(50) C. Schröder, T. Rudas, G. Neumayr, S. Benkner, O. Steinhauser, On the collective

network of ionic liquid/water mixtures. I. Orientational structure, J. Chem. Phys. **127**, 234503 (2007).

(51) A. Heintz, J.K. Lehmann, C. Wertz, J. Jacquemin, Thermodynamic properties of mixtures containing ionic liquids. 4. LLE of binary mixtures of [C_2MIM][NTf2] with propan-1-ol, butan-1-ol, and pentan-1-ol and [C_2MIM][NTf2] with cyclohexanol and 1,2-hexanediol including studies of the influence of small amounts of water. J. Chem.Eng. Data. **50**, 956 (2005).

Figures

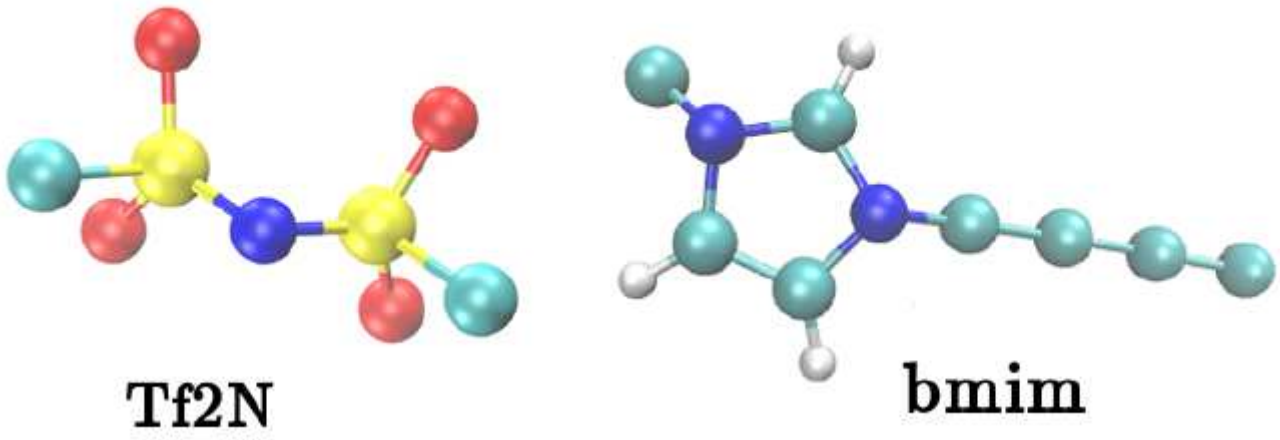

Figure 1

The cyan spheres represent a Carbon atom, red spheres a Oxygen atom, blue spheres a Sodium atom, yellow spheres a Sulfur atom and white spheres Hidrogen (only the carbons at the aromatic ring have an explicit hidrogen), the contribution of the other Hydrogen atoms is contained in the respective carbons, as well as the contribution of the Fluorine atoms.

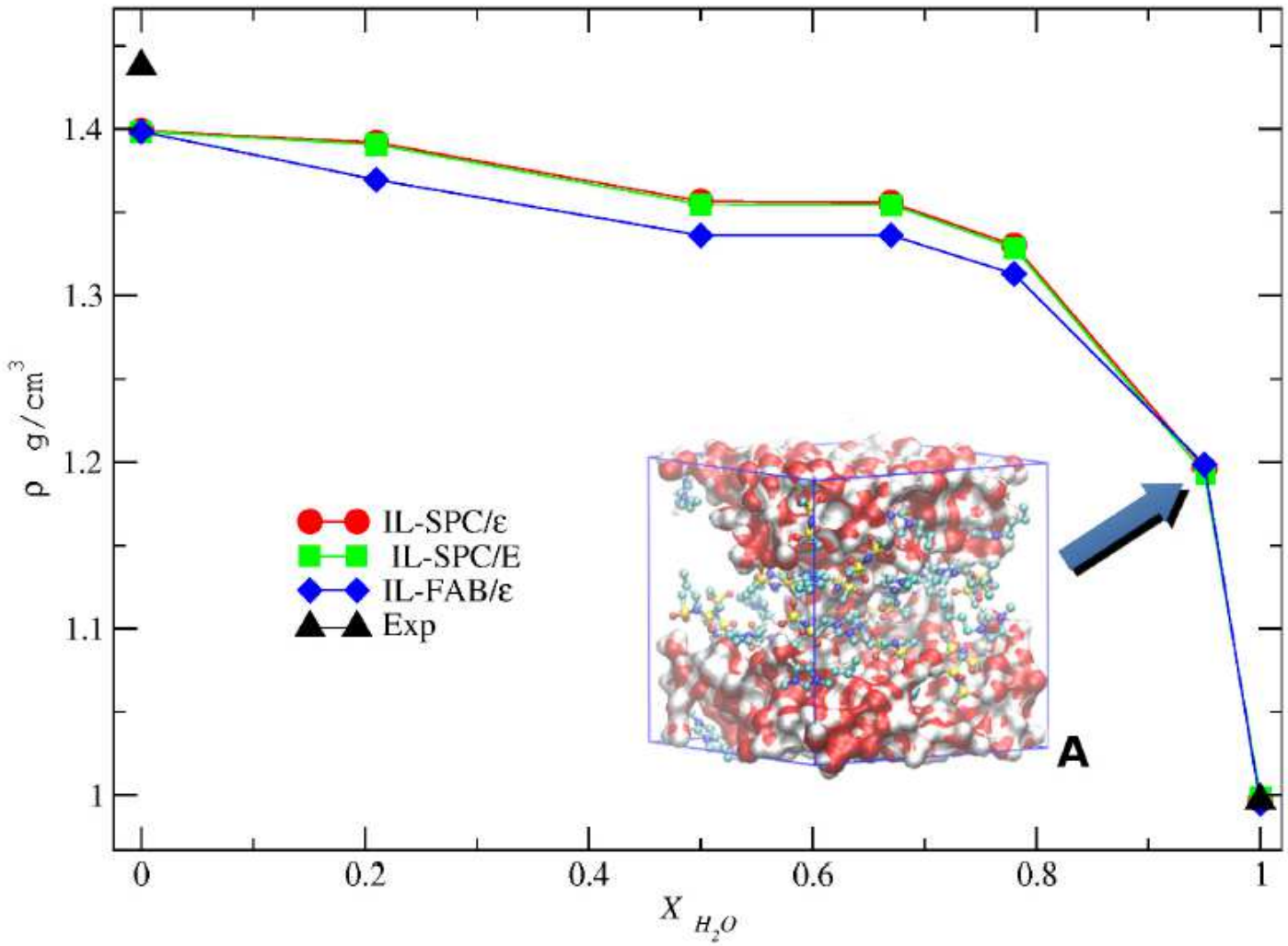

Figure 2

Density of the water-IL solution as function of the molar fraction of water at 1 bar of pressure. Black triangles are the experimental data,44 red circles are the result using the SPC/ε model, green box are the result using the SPC/E model, and the blue dimonds are the result using FAB/ε model, all calculated in this work.

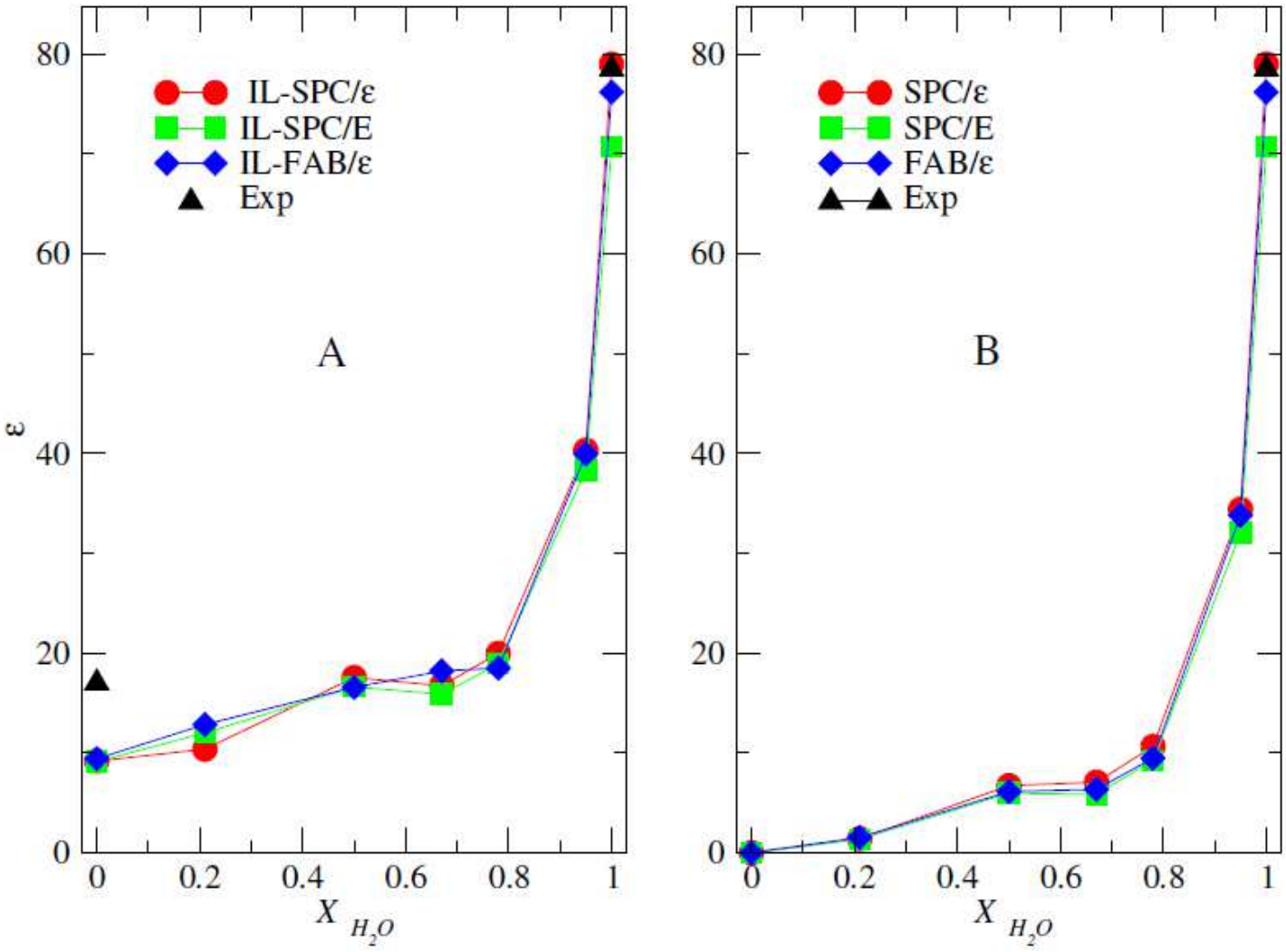

Figure 3

A: Dielectric constant of the water-IL solution as function of the molar fraction of water. B: Dielectric constant of the water in the IL-water solution as function of the molar fraction of water. Both at 1 bar of pressure and 298 K of temperature. Black triangles are the experimental data,45 red circles are the result using the SPC/ model, green box are the result using the SPC/E model and the blue dimonds are the result using FAB/ model, all calculated in this work.

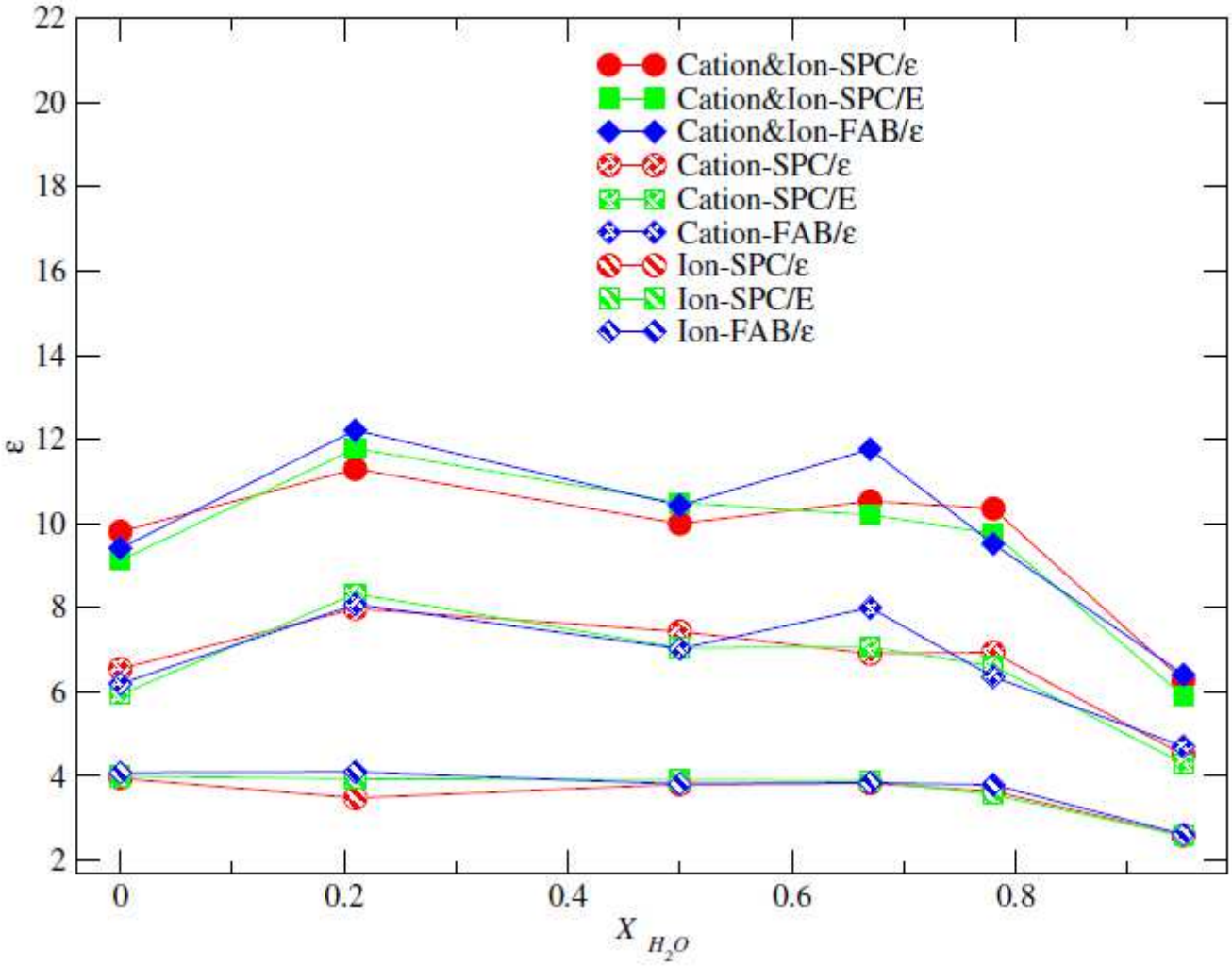

Figure 4

Dielectric constant of the IL, cation and anion in the water-IL solution as function of the molar fraction of water at 1 bar of pressure.

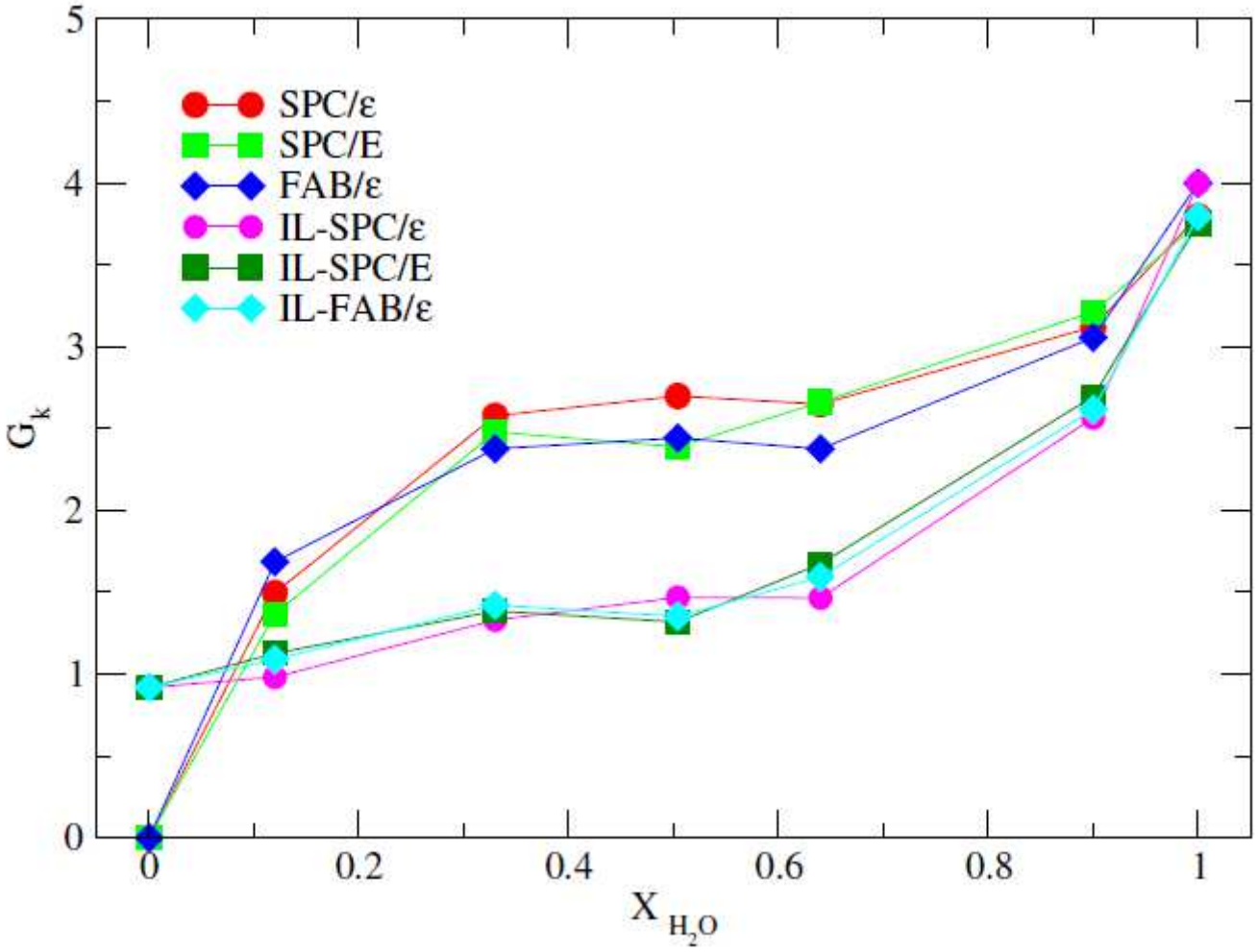

Figure 5

Kirkwood factor GK of the water in the IL-water solution and for all solution as function of the molar fraction of water at 1 bar of pressure and 300K. Red circles are the result using the SPC/ε model, green box are the result using the SPC/E model and the blue dimonds are the result using FAB/ε model, all calculated in this work.

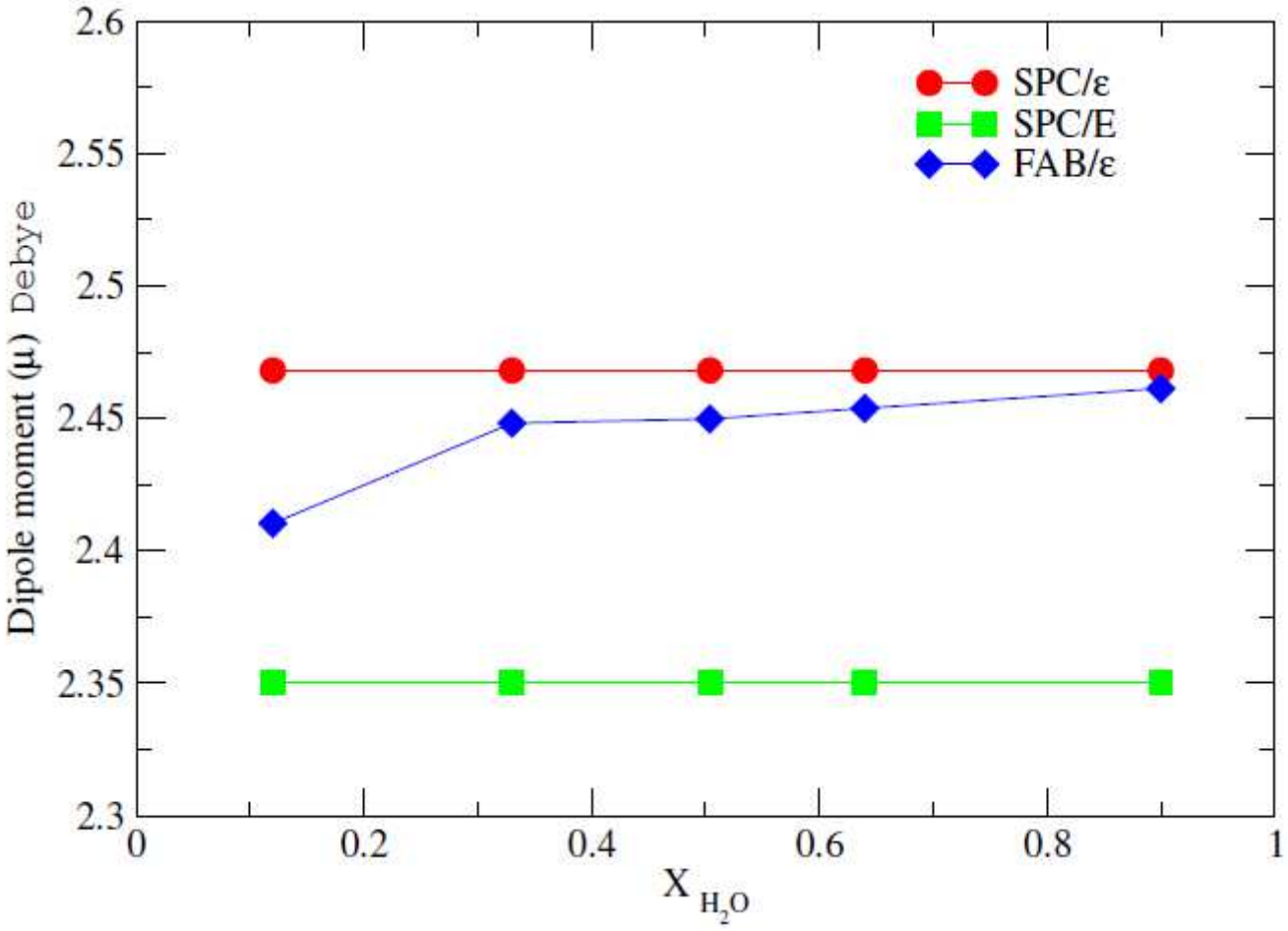

Figure 6

Dipole Moment of the water in the IL-water solution as function of the molar fraction of water at 1 bar of pressure and 300K. Red circles are the result using the SPC/ε model, green box are the result using the SPC/E model and the blue dimonds are the result using FAB/ε model, all calculated in this work.

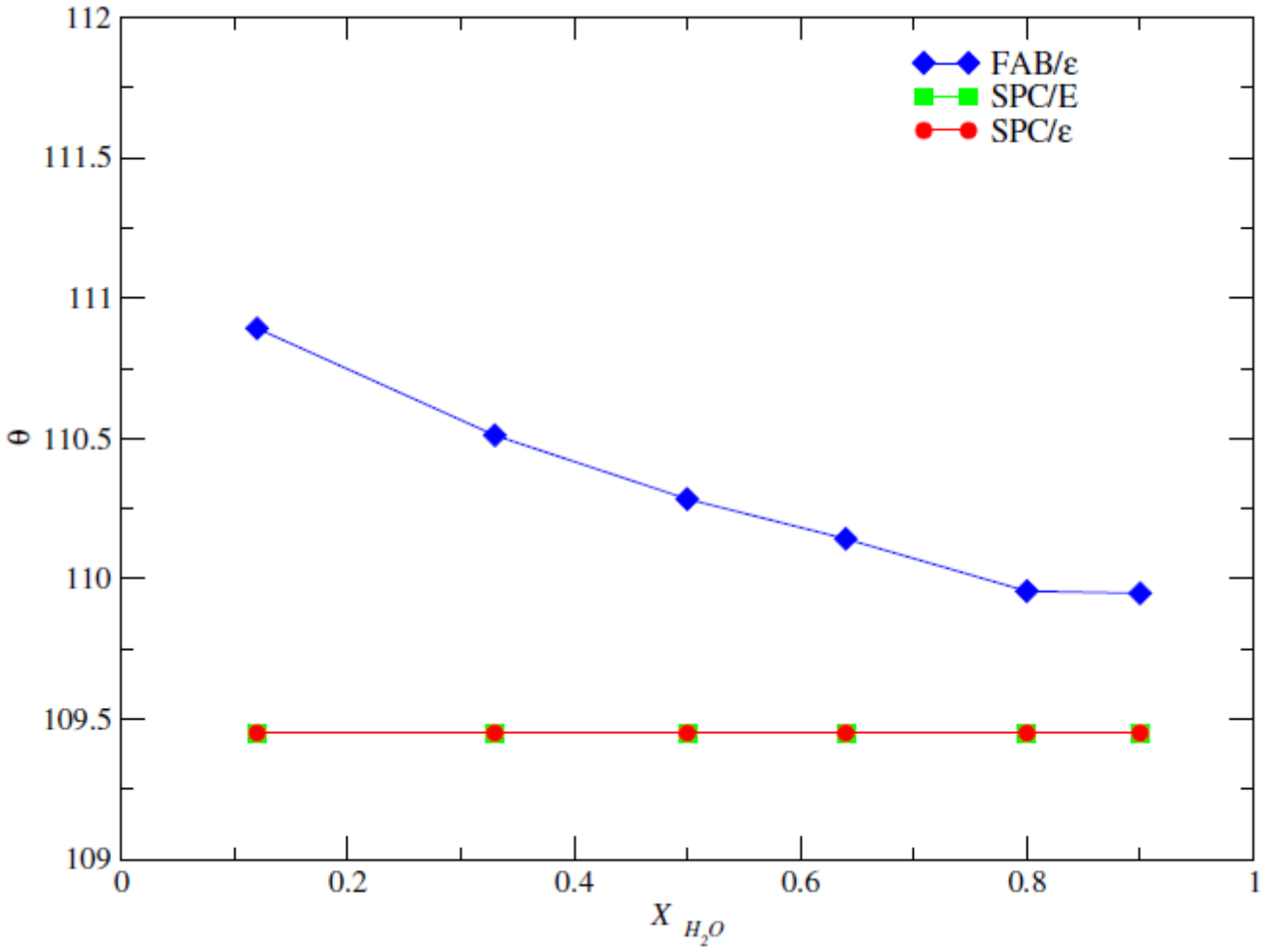

Figure 7

Average angle of the water described by the three force fields as function of the molar fraction of water at 1 bar of pressure and 300K. Red circles are the result using the SPC/ε model, green box are the result using the SPC/E model and the blue dimonds are the result using FAB/ε model, all calculated in this work.

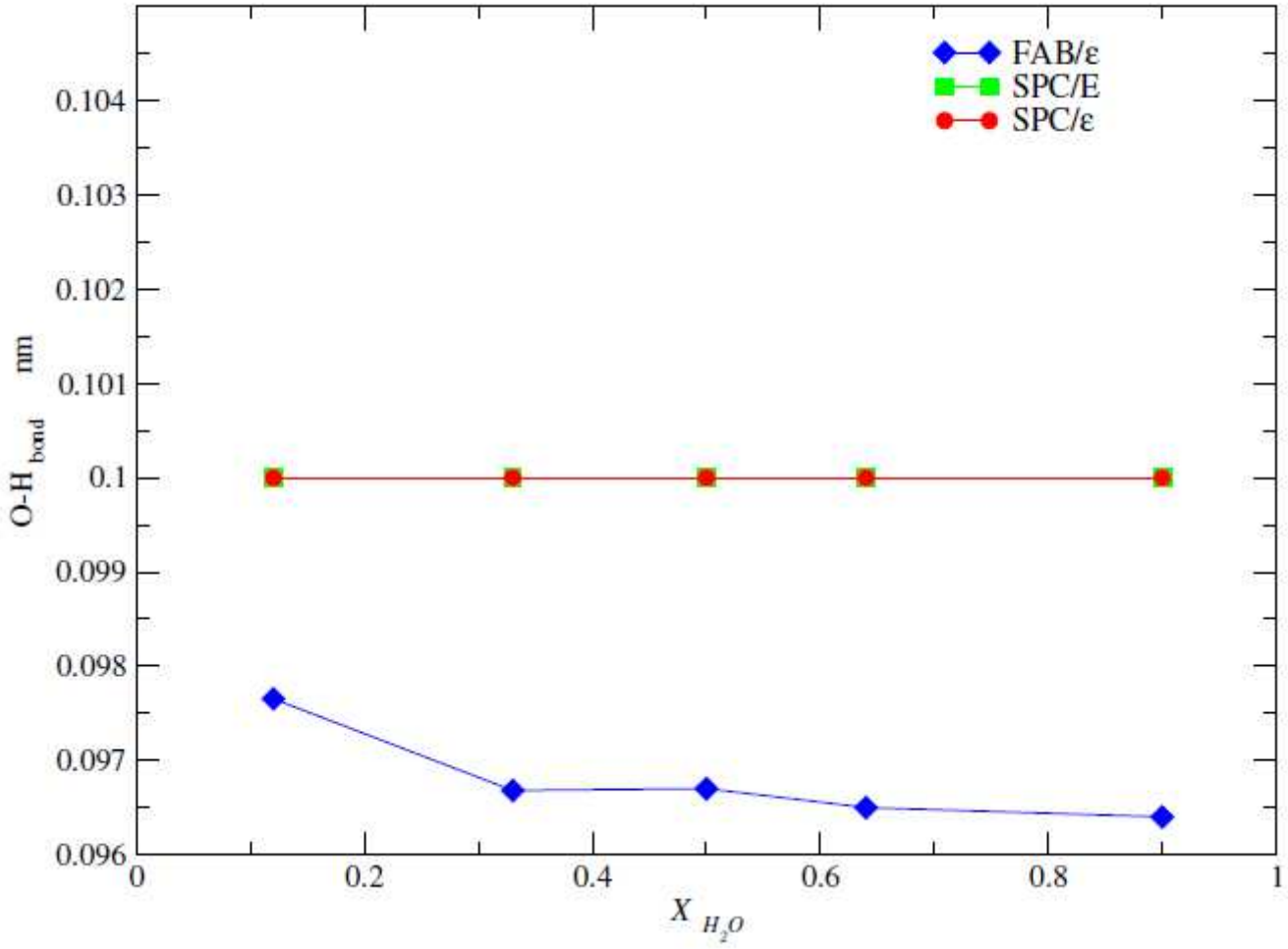

Figure 8

Average O-Hbond of the water described by the three force fields as function of the molar fraction of water at 1 bar of pressure and 300K. Red circles are the result using the SPC/ε model, green box are the result using the SPC/E model and the blue dimonds are the result using FAB/ε model, all calculated in this work.

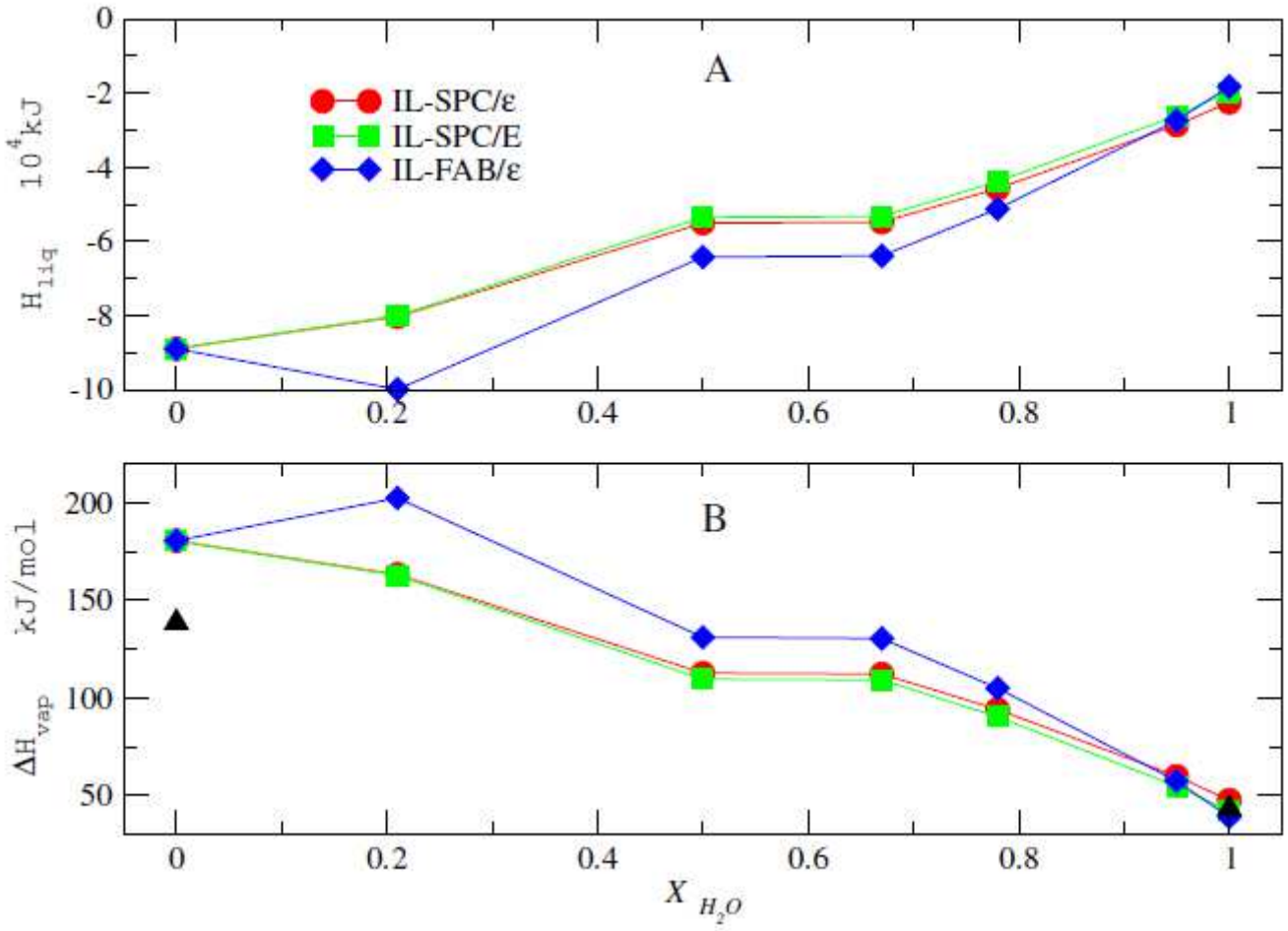

Figure 9

A. Enthalpy of the liquid phase the IL-water solution as function of the molar fraction of water. B. ΔHvap of the system with respect to the fraction of water in the solution IL-water. Both at 1 bar of pressure and 300K of temperature. Black triangles are the experimental data,48 red circles are the result using the SPC/ □ model, green box are the result using the SPC/E model and the blue dimonds are the result using FAB/□ model, all calculated in this work.

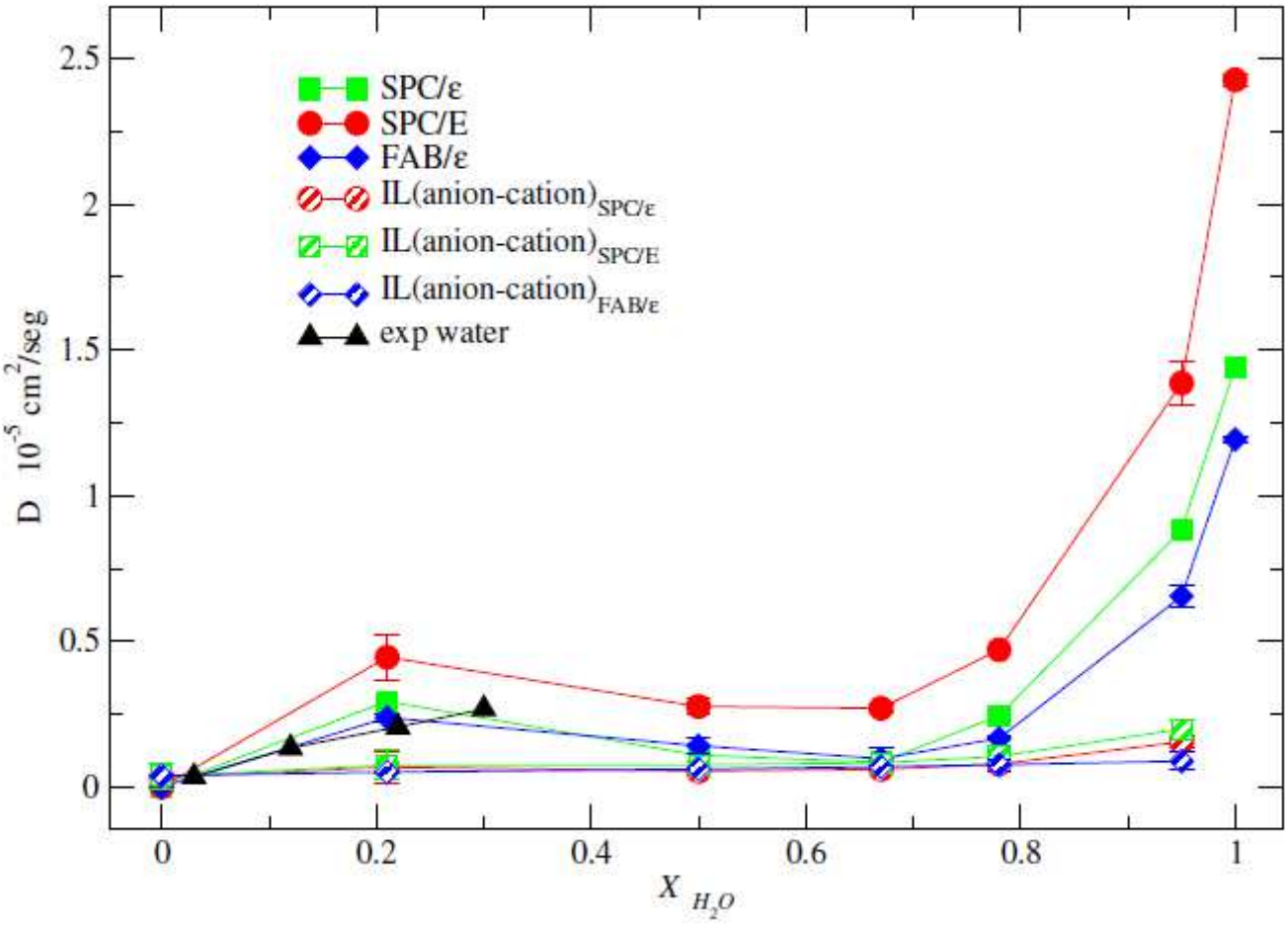

Figure 10

The self-diffusion coefficients of water and the IL with respect to the fraction of water in the solution IL-water. Black triangles are the experimental data,25 red circles are the result using the SPC/ model, green box are the result using the SPC/E model and the blue dimonds are the result using FAB/ model, all calculated in this work.

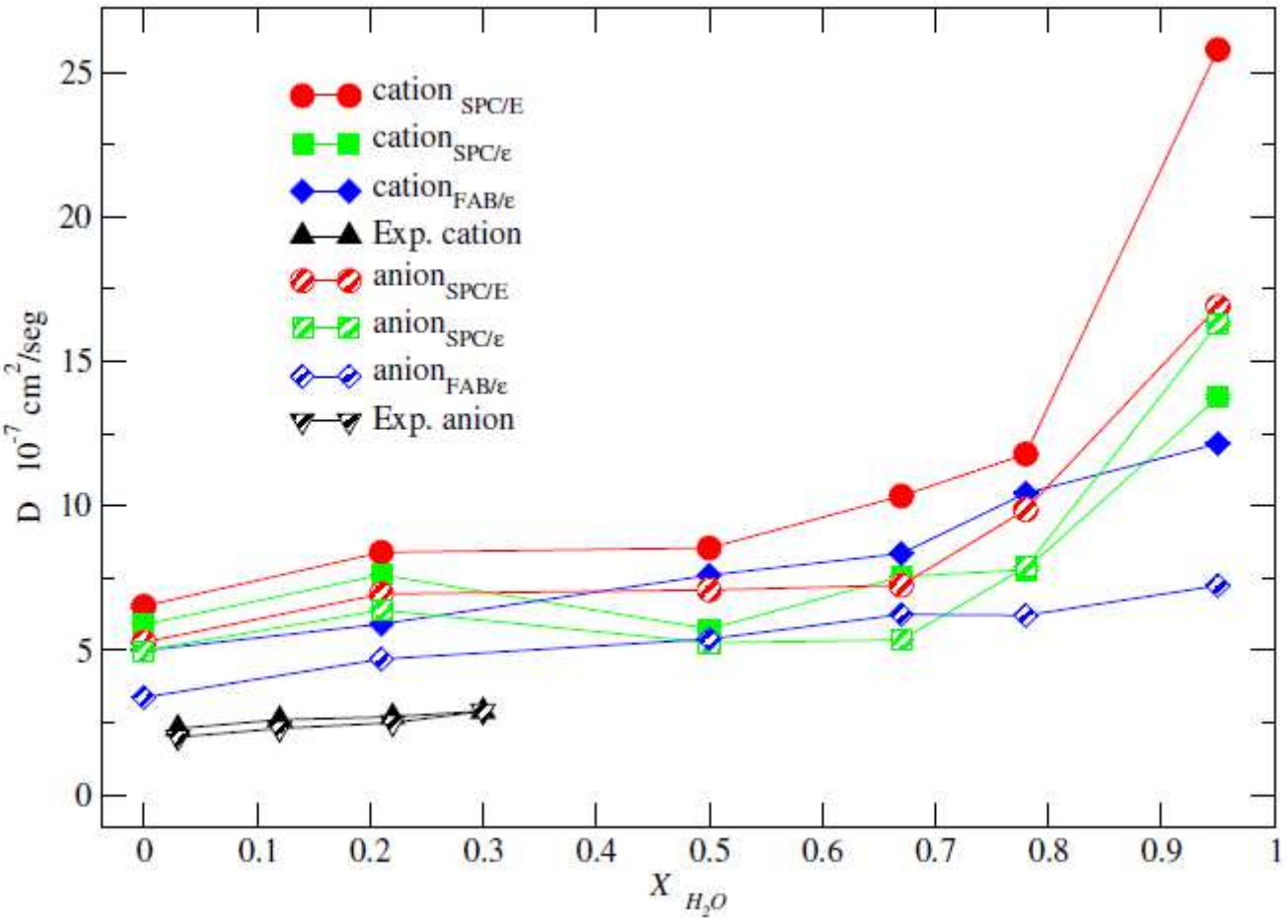

Figure 11

The self-diffusion coefficients of anion and the cation with respect to the fraction of water in the solution IL-water. Black triangles are the experimental data,25 red circles are the result using the SPC/ model, green box are the result using the SPC/E model and the blue dimonds are the result using FAB/ model, all calculated in this work.

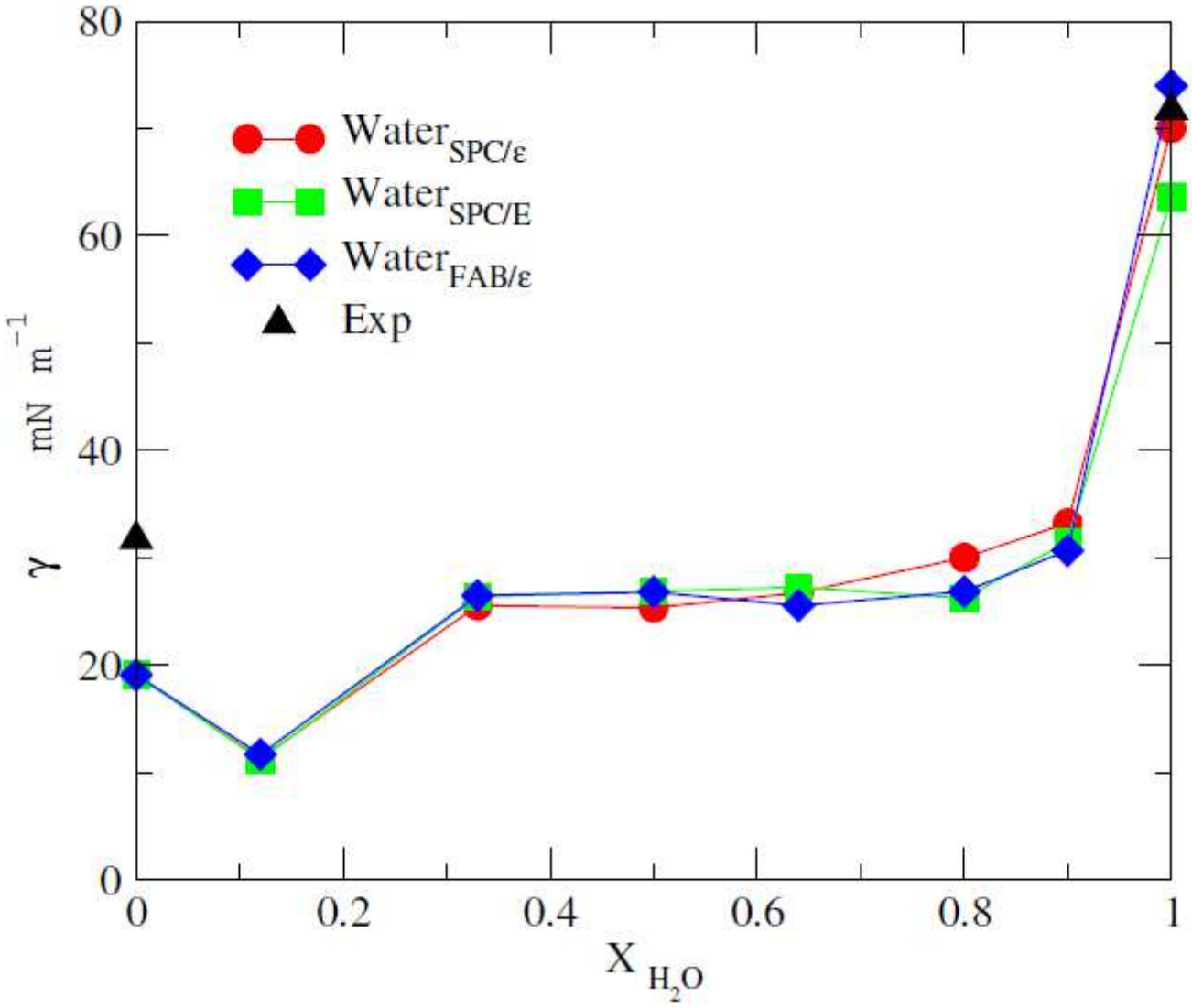

Figure 12

The surface tension of the system with respect to the fraction of water in the solution IL-water. Black triangles are the experimental data,25 red circles are the result using the SPC/ε model, green box are the result using the SPC/E model and the blue dimonds are the result using FAB/ε model, all calculated in this work.